

DYNAMIC TRANSITIONS OF QUASI-GEOSTROPHIC CHANNEL FLOW

HENK DIJKSTRA, TAYLAN SENGUL, JIE SHEN, AND SHOUHONG WANG

ABSTRACT. The main aim of this paper is to describe the dynamic transitions in flows described by the two-dimensional, barotropic vorticity equation in a periodic zonal channel. In [3], the existence of a Hopf bifurcation in this model as the Reynolds number crosses a critical value was proven. In this paper, we extend the results in [3] by addressing the stability problem of the bifurcated periodic solutions. Our main result is the explicit expression of a non-dimensional number γ which controls the transition behavior. We prove that depending on γ , the modeled flow exhibits either a continuous (Type I) or catastrophic (Type II) transition. Numerical evaluation of γ for a physically realistic region of parameter space suggest that a catastrophic transition is preferred in this flow.

1. INTRODUCTION

Climate variability exhibits recurrent large-scale patterns which are directly linked to dynamical processes represented in the governing dissipative dynamical system [6, 7, 8]. The study of the persistence of these patterns and the transitions between them also play a crucial role in understanding climate change and in interpreting future climate projections [9].

Current climate models used for developing such projections are based on the conservation laws of fluid mechanics and consist of systems of nonlinear partial differential equations (PDEs). These can be put into the perspective of infinite-dimensional dissipative systems exhibiting large-dimensional attractors. The global attractor is a mathematical object strongly connected to the overall dissipation in the system. Climate variability is, however, often associated with dynamic transitions between different regimes, each represented by local attractors.

There are many examples of climate phenomena where such transitions have been investigated numerically, such as the transition to oscillatory behavior in models of the El Niño/Southern Oscillation phenomenon in the equatorial Pacific, the transitions between different mean flow patterns of the Kuroshio Current in the North Pacific and the transitions between blocked and zonal flows in the midlatitude atmosphere (see, e.g., [5]). However, rigorous mathematical results on the type of the transitions in these systems of PDEs are extremely scarce.

This paper arises out of a research program to generate rigorous mathematical results on climate variability developed from the viewpoint of dynamical transitions. We have shown [10] that the transitions of all dissipative systems can be classified into three classes: continuous, catastrophic and random, which correspond to very different dynamical transition behavior of the system.

Key words and phrases. quasi-geostrophic flow, channel flow, spatial-temporal patterns, dynamic transitions, climate variability.

We here focus on the dynamic transitions in flows described by one of the cornerstone dynamical models in both oceanic and atmospheric dynamics, the two-dimensional, dimensionless barotropic vorticity equation given by

$$(1.1) \quad \frac{\partial \Delta \psi}{\partial t} + \epsilon J(\psi, \Delta \psi) + \frac{\partial \psi}{\partial x} = E \Delta^2 \psi + \alpha_\tau \sin \pi y,$$

where Δ is the Laplacian operator, $J(F, G) = (\partial F / \partial x)(\partial G / \partial y) - (\partial F / \partial y)(\partial G / \partial x)$ is the advection operator and ψ the geostrophic stream function. The equation (1.1) describes flows with a typical length scale L on a mid-latitude beta-plane with a central latitude θ_0 and a planetary vorticity gradient β_0 . It can be derived from the primitive equations by the so-called quasi-geostrophic (QG) approximation, which assumes a dominant balance between the Coriolis force and the pressure gradient force [11].

To derive (1.1), time, length and stream function were non-dimensionalised with $1/(\beta_0 L)$, L and UL , where U is a characteristic horizontal velocity. The positive parameters ϵ and E are Rossby and Ekman numbers, respectively, given by

$$\epsilon = \frac{U}{\beta_0 L^2}; \quad E = \frac{A_H}{\beta_0 L^3}$$

where A_H is the lateral friction coefficient. The Reynolds number R is defined as

$$(1.2) \quad R = \frac{\epsilon}{E} = \frac{UL}{A_H}$$

The forcing term $\alpha_\tau \sin \pi y$ in (1.1) may represent the transfer of angular momentum into midlatitudes due to tropical Hadley cell in an atmospheric model. In this case, the magnitude of the velocity can be scaled such that $\alpha_\tau = 1$. In the ocean case, the forcing term represents the dimensionless wind stress

$$\tau = \frac{\alpha_\tau}{\pi} (\cos \pi y, 0)$$

Such a wind stress mimics the annually averaged zonal wind distribution over the North Atlantic and North Pacific with westerly (i.e. eastward) winds over the midlatitudes and easterlies in the tropics and polar latitudes. When the dimensionless wind stress has a magnitude τ_0 and the ocean basin a depth D and the water a density ρ , the factor α_τ is given by

$$\alpha_\tau = \frac{\tau_0}{\rho D L \beta_0 U}$$

In this case, we can choose U such that $\alpha_\tau = 1$, which is usually referred to as the Sverdrup scaling. In both ocean and atmosphere cases the equation (1.1) has two free parameters (out of the three ϵ , E and R) which we choose here as R and E .

We consider flows in a so-called zonal channel of length $2/a$ with walls bounding the domain at $y = \pm 1$ and periodic conditions in zonal direction. The equation (1.1) is therefore supplemented with boundary conditions

$$(1.3) \quad \begin{aligned} \psi|_{x=0} &= \psi|_{x=2/a}, \\ \psi|_{y=\pm 1} &= \frac{\partial^2 \psi}{\partial y^2} |_{y=\pm 1} = 0. \end{aligned}$$

The equations (1.1) with (1.3) admit the following steady state

$$(1.4) \quad \psi_0 = -\frac{1}{\pi^4 E} \sin \pi y,$$

which represents a zonal jet with zonal velocity field $u_0 = -\partial\psi_0/\partial y = 1/(\pi^3 E) \cos \pi y$.

It is shown in [3] that for any $a \geq \sqrt{3}/2$, ψ_0 is both linearly and nonlinearly stable. Also, there is an α_0 with $\sqrt{3}/4 < \alpha_0 < \sqrt{3}/2$ such that for any $\sqrt{3}/4 \leq a \leq \alpha_0$, there is a critical Reynolds number $R_0 > 0$ depending on a such that a simple pair of complex conjugate eigenvalues cross the imaginary axis as the Reynolds number R crosses R_0 , leading to the existence of Hopf bifurcation at the critical Reynolds number. However, the stability of the bifurcated periodic solutions and the dynamic transition behavior near R_0 are so far unknown. The main difficulty is caused by the lack of explicit analytical form of the eigenfunctions.

The main objective of this article is to investigate the dynamic transition and the stability of the basic state (1.4) as the Reynolds number crosses a critical threshold R_0 . The main result we obtain is that the dynamic transition from this state to new states is either continuous (Type-I) or catastrophic (Type-II), and is determined by the sign of a computable parameter γ given by (2.10). Our numerical investigations indicate that in a physically relevant parameter regime, only catastrophic transitions occur.

2. MAIN THEOREM

Throughout $\operatorname{Re} z$, $\operatorname{Im} z$, \bar{z} will denote the real part, imaginary part and conjugate of a complex number z . $D = \frac{d}{dy}$ is the derivative operator, $\Omega = (0, 2/a) \times (-1, 1) \subset \mathbb{R}^2$ and (\cdot, \cdot) is the $L^2(\Omega)$ inner product.

2.1. Functional setting. Considering the deviation $\psi' = \psi - \psi_0$ from the basic steady state (1.4) and omitting the primes, we obtain from (1.1),

$$(2.1) \quad \frac{\partial \Delta \psi}{\partial t} + \epsilon J(\psi, \Delta \psi) = -\frac{R}{\pi^3} \cos \pi y \left(\Delta \frac{\partial \psi}{\partial x} + \pi^2 \frac{\partial \psi}{\partial x} \right) - \frac{\partial \psi}{\partial x} + E \Delta^2 \psi.$$

Note that (1.1) can also be formulated in velocity $\mathbf{u} = \left(-\frac{\partial \psi}{\partial y}, \frac{\partial \psi}{\partial x} \right)$ and pressure p as

$$(2.2) \quad \begin{aligned} \frac{\partial \mathbf{u}}{\partial t} + \epsilon (\mathbf{u} \cdot \nabla) \mathbf{u} + f \mathbf{k} \times \mathbf{u} &= E \Delta \mathbf{u} - \nabla p + \tau, \\ \nabla \cdot \mathbf{u} &= 0. \end{aligned}$$

Here f is the dimensionless Coriolis parameter on a midlatitude beta plane that gives rise to the $\partial\psi/\partial x$ term in (1.1); \mathbf{k} is the unit vector in the z -direction.

Using the formulation (2.2), we can write the problem in the following abstract form

$$(2.3) \quad \frac{d\mathbf{u}}{dt} = L\mathbf{u} + G(\mathbf{u}),$$

where $L : H_1 \rightarrow H$ is the linear operator, $G : H_1 \rightarrow H$ is the nonlinear operator, and

$$\begin{aligned} H &= \{ \mathbf{u} = (u, v) \in (L_2(\Omega))^2 \mid v|_{y=\pm 1} = 0, \operatorname{div} \mathbf{u} = 0, \mathbf{u}|_{x=0} = \mathbf{u}|_{x=2/a} \} \\ H_1 &= H \cap (H^1(\Omega))^2. \end{aligned}$$

The eigenvalue problem for the linearized equation of (2.1) reads

$$(2.4) \quad E \Delta^2 \psi + \frac{R}{\pi^3} \cos(\pi y) (\Delta \psi_x + \pi^2 \psi_x) - \psi_x = \beta \Delta \psi$$

with boundary conditions (1.3).

Since the solution ψ is periodic in x with period $2/a$, we can expand ψ in Fourier series, so for the m -mode of the expansion, we can write

$$(2.5) \quad \psi = e^{i\alpha_m x} Y(y), \quad \alpha_m = am\pi.$$

where $Y(y)$ satisfies the boundary condition $Y(\pm 1) = D^2 Y(\pm 1) = 0$. Plugging (2.5) into (2.4), we obtain a sequence of one-dimensional problem:

$$(2.6) \quad E(D^2 - \alpha_m^2)^2 Y + i\alpha_m \left(\frac{R}{\pi^3} \cos(\pi y) (D^2 - \alpha_m^2 + \pi^2) - 1 \right) Y = \beta(D^2 - \alpha_m^2) Y.$$

The eigenvectors of (2.4) are $\psi_{m,j} = e^{i\alpha_m x} Y_{m,j}(y)$ where $Y_{m,j}$ are the eigenvectors of (2.6) corresponding to the eigenvalues $\beta_{m,j} \in \mathbb{C}$ where $m \in \mathbb{Z}$, $j = 1, 2, 3, \dots$. Moreover $\beta_{m,j}$ are ordered so that $\text{Re } \beta_{m,j} \leq \text{Re } \beta_{m,k}$ if $j > k$. Also $\beta_{-m,j} = \overline{\beta_{m,j}}$ and we can take $\psi_{-m,j} = \overline{\psi_{m,j}}$. In particular $\psi_{0,j}$ and $\beta_{0,j}$ are real.

We also need to consider the eigenvalue problem for the adjoint linear operator which can be written as

$$E\Delta^2 \psi^* - \frac{R}{\pi^3} \Delta(\cos(\pi y) \psi_x^*) - \frac{R}{\pi^3} \pi^2 \cos(\pi y) \psi_x^* + \psi_x^* = \beta \Delta \psi^*.$$

Using $\psi^* = e^{i\alpha_m x} Y^*(y)$, we obtain the analog of (2.6)

$$(2.7) \quad \begin{aligned} E(D^2 - \alpha_m^2)^2 Y^* - i\alpha_m \left(\frac{R}{\pi^3} D^2(Y^* \cos(\pi y)) + \frac{R}{\pi^3} \cos(\pi y) (\pi^2 - \alpha_m^2) Y^* - Y^* \right) \\ = \beta^*(D^2 - \alpha_m^2) Y^*. \end{aligned}$$

By basic properties of the adjoint linear eigenvalue problem, we have $\beta_{m,j}^* = \overline{\beta_{m,j}}$ and

$$(2.8) \quad (\mathbf{u}_{m,j}, \mathbf{u}_{n,k}^*) = 0, \quad \text{if } (m, j) \neq (n, k),$$

where $\mathbf{u}_{m,j} = \left(\frac{\partial}{\partial y}, -\frac{\partial}{\partial x} \right) \psi_{m,j}$.

2.2. The main theorem and its proof. Our main aim is to identify the transitions of (2.1) in the case where two complex conjugate eigenvalues cross the imaginary axis. Thus, we assume the following condition on the spectrum of the linearized operator.

Assumption 1. *Depending on a and E , there exists a critical Reynolds number R_0 and a zonal wave integer $m_0 \geq 1$ such that*

$$\begin{aligned} \text{Re}(\beta_{m_0,1}(R)) = \text{Re}(\beta_{-m_0,1}(R)) = \begin{cases} < 0 & \text{if } R < R_0, \\ = 0 & \text{if } R = R_0, \\ > 0 & \text{if } R > R_0. \end{cases} \\ \text{Re}(\beta_{m,j}(R_0)) < 0, \quad \text{if } (m, j) \neq (\pm m_0, 1). \end{aligned}$$

In [3], the validity of the Assumption 1 is shown with $m_0 = 1$ when $\sqrt{3}/4 \leq a \leq \alpha_0$ for some $\sqrt{3}/4 < \alpha_0 < \sqrt{3}/2$.

Let us define

$$\begin{aligned}
I_1 &= \int_{-1}^1 \overline{Y_{m_0,1}^*}(y) ((am_0\pi)^2 - D^2) Y_{m_0,1}(y) dy, \\
(2.9) \quad I_2(k) &= \int_{-1}^1 \cos(k\pi y) Y_{m_0,1}^*(y) ((am_0\pi)^2 - k^2\pi^2 - D^2) \overline{Y_{m_0,1}}(y) dy, \\
I_3(k) &= \int_{-1}^1 \sin(k\pi y) Y_{m_0,1}(y) D\overline{Y_{m_0,1}}(y) dy.
\end{aligned}$$

where $Y_{m_0,1}$ and $Y_{m_0,1}^*$ are solutions of (2.6) and (2.7) respectively for $m = m_0$, at $R = R_0$.

We define the transition number

$$(2.10) \quad \gamma = -\frac{E(R_0 am_0)^2 \pi}{2|I_1|^2} \sum_{k=1}^{\infty} \frac{\text{Im } I_3(k) \text{Im}\{I_1 I_2(k)\}}{k}.$$

As the next theorem shows, the sign of γ determines the type of transition of the system at the critical Reynolds number R_0 .

Theorem 1. *Let γ be defined by (2.10) and let*

$$(2.11) \quad \mathbf{u}_{bif}(t, x, y) = \sqrt{\frac{-\text{Re } \beta_{m_0,1}}{\gamma}} \text{Re} \left(e^{it \text{Im } \beta_{m_0,1}} \mathbf{u}_{m_0,1}(x, y) \right) + o(\sqrt{|\text{Re } \beta_{m_0,1}|}).$$

Under the Assumption 1, the following assertions hold true:

- (1) *If $\gamma < 0$ then the problem undergoes a Type-I (continuous) transition at $R = R_0$ and bifurcates to the time periodic solution \mathbf{u}_{bif} on $R > R_0$ which is an attractor.*
- (2) *If $\gamma > 0$ then the problem undergoes a Type-II (catastrophic) transition at $R = R_0$ and bifurcates to the time periodic solution \mathbf{u}_{bif} on $R < R_0$ which is a repeller.*

Proof. Let $\mathbf{u}_{m_0,1} = (\frac{\partial}{\partial y}, -\frac{\partial}{\partial x})\psi_{m_0,1}$ where $\psi_{m_0,1} = e^{iam_0\pi x} Y_{m_0,1}(y)$, denote the first critical eigenfunction corresponding to the eigenvalue $\beta_{m_0,1}$ in Assumption (1). For simplicity of notation, we will denote

$$\begin{aligned}
(2.12) \quad \mathbf{u}^1 &= \text{Re } \mathbf{u}_{m_0,1}, & \mathbf{u}^2 &= \text{Im } \mathbf{u}_{m_0,1}, \\
\psi^1 &= \text{Re } \psi_{m_0,1}, & \psi^2 &= \text{Im } \psi_{m_0,1}, \\
Y^1 &= \text{Re } Y_{m_0,1}, & Y^2 &= \text{Im } Y_{m_0,1},
\end{aligned}$$

where $Y_{m_0,1}$ solves equation (2.6).

In the proof we will use the following trilinear operators

$$(2.13) \quad G(\mathbf{u}_I, \mathbf{u}_J, \mathbf{u}_K) = -\epsilon \int_{\Omega} (\mathbf{u}_I \cdot \nabla) \mathbf{u}_J \cdot \overline{\mathbf{u}_K} dx dy.$$

and

$$G_s(\mathbf{u}_I, \mathbf{u}_J, \mathbf{u}_K) = G(\mathbf{u}_I, \mathbf{u}_J, \mathbf{u}_K) + G(\mathbf{u}_J, \mathbf{u}_I, \mathbf{u}_K).$$

Step 1. Computation of nonlinear interactions. It is easy to see that only $(0, k)$ and $(2m, k)$ adjoint modes interact nonlinearly with the critical $(m_0, 1)$ -mode i.e.

$$(2.14) \quad G(\mathbf{u}^i, \mathbf{u}^j, \mathbf{u}_{n,k}^*) = 0 \quad \text{if } n \neq 0, \text{ or } n \neq 2m, i, j = 1, 2.$$

We will first investigate these interactions. We have $\mathbf{u}_{0k} = \mathbf{u}_{0k}^* = (\frac{\partial}{\partial y}\psi_{0k}, 0) = (DY_{0k}, 0)$ where Y_{0k} is given by (2.42). In particular \mathbf{u}_{0k}^* is real. Using

$$G(\mathbf{u}, \mathbf{u}, \mathbf{u}_{0k}^*) = C \int_{x=0}^{2/a} e^{2iam_0\pi x} dx = 0,$$

where $C = \int_{y=-1}^1$ (only y -dependent terms) dy , we get

$$(2.15) \quad 0 = G(\mathbf{u}^1, \mathbf{u}^1, \mathbf{u}_{0k}^*) - G(\mathbf{u}^2, \mathbf{u}^2, \mathbf{u}_{0k}^*) + i(G(\mathbf{u}^1, \mathbf{u}^2, \mathbf{u}_{0k}^*) + G(\mathbf{u}^2, \mathbf{u}^1, \mathbf{u}_{0k}^*))$$

Also noting,

$$G(\bar{\mathbf{u}}, \mathbf{u}, \mathbf{u}_{2m,k}^{*l}) = C \int_{x=0}^{2/a} e^{-i\alpha_{m_0}x} e^{i\alpha_{m_0}x} T(\alpha_{2m}x) dx = 0,$$

where $C = \int_{y=-1}^1$ (only y -dependent terms) dy and $T = \sin$ or $T = \cos$, we get

$$(2.16) \quad 0 = G(\mathbf{u}^1, \mathbf{u}^1, \mathbf{u}_{2m,k}^{*l}) + G(\mathbf{u}^2, \mathbf{u}^2, \mathbf{u}_{2m,k}^{*l}) + i(G(\mathbf{u}^1, \mathbf{u}^2, \mathbf{u}_{2m,k}^{*l}) - G(\mathbf{u}^2, \mathbf{u}^1, \mathbf{u}_{2m,k}^{*l}))$$

Let us define

$$(2.17) \quad \begin{aligned} g_{0k}^{ij} &= G(\mathbf{u}^i, \mathbf{u}^j, \mathbf{u}_{0k}^*), \\ g_{2m,k}^{ij} &= G(\mathbf{u}^i, \mathbf{u}^j, \mathbf{u}_{2m,k}^{*l}). \end{aligned}$$

(2.15),(2.16) and (2.17) imply that

$$(2.18) \quad \begin{aligned} g_{0k}^{11} &= g_{0k}^{22}, & g_{0k}^{12} &= -g_{0k}^{21}, \\ g_{2m,k}^{11} &= -g_{2m,k}^{22}, & g_{2m,k}^{12} &= g_{2m,k}^{21}. \end{aligned}$$

A lengthy but straightforward calculation which can also be verified by a symbolic computation software shows that

$$\begin{aligned} G(\mathbf{u}^1, \mathbf{u}^1, \mathbf{u}_{2m,k}^{*1}) &= G(\mathbf{u}^1, \mathbf{u}^2, \mathbf{u}_{2m,k}^{*2}), \\ G(\mathbf{u}^1, \mathbf{u}^1, \mathbf{u}_{2m,k}^{*2}) &= -G(\mathbf{u}^1, \mathbf{u}^2, \mathbf{u}_{2m,k}^{*1}), \end{aligned}$$

which implies that

$$(2.19) \quad g_{2m,k}^{11} = ig_{2m,k}^{12}.$$

Step 2. Approximation of the center manifold. Next we obtain an approximation for the center manifold function Φ . Let $H = E_1 \oplus E_2$, $E_1 = \text{span}\{\mathbf{u}^1, \mathbf{u}^2\}$, $E_2 = E_1^\perp$. By [10], near $R = R_0$, the center manifold Φ can be approximated by the formula

$$(2.20) \quad \begin{aligned} ((-\mathcal{L})^2 + 4\text{Im}(\beta)^2)(-\mathcal{L})\Phi &= ((-\mathcal{L})^2 + 2\text{Im}(\beta)^2)P_2G(x_1\mathbf{u}^1 + x_2\mathbf{u}^2) \\ &+ 2\text{Im}(\beta)^2P_2G(x_1\mathbf{u}^2 - x_2\mathbf{u}^1) \\ &+ \text{Im}(\beta)(-\mathcal{L})G(x_1\mathbf{u}^1 + x_2\mathbf{u}^2, x_2\mathbf{u}^1 - x_1\mathbf{u}^2) \\ &+ \text{Im}(\beta)(-\mathcal{L})G(x_2\mathbf{u}^1 - x_1\mathbf{u}^2, x_1\mathbf{u}^1 + x_2\mathbf{u}^2) + o(2), \end{aligned}$$

where

$$o(2) = o(x_1^2 + x_2^2) + O(|\text{Re } \beta(R)|(x_1^2 + x_2^2)).$$

Here $\mathcal{L} = L|_{E_2}$ is the projection of the linear operator L onto E_2 .
Let us write

$$\Phi = \sum_J \Phi_J \mathbf{u}_J.$$

Note that for an eigenvector \mathbf{u}_K^* of L^* corresponding to $\beta_K^* = \bar{\beta}_K$, by orthogonality relation (2.8), we have

$$\begin{aligned} ((-\mathcal{L})^2 + 4 \operatorname{Im}(\beta)^2)(-\mathcal{L})\Phi, \mathbf{u}_K^* &= \sum_K -\Phi_J \beta_K (\beta_K^2 + 4 \operatorname{Im}(\beta)^2)(\mathbf{u}_J, \mathbf{u}_K^*) \\ &= m_K \Phi_K, \end{aligned}$$

where

$$m_K = -\beta_K (\beta_K^2 + 4 \operatorname{Im}(\beta)^2)(\mathbf{u}_K, \mathbf{u}_K^*).$$

By (2.14) and the center manifold formula (2.20), we have the following approximation for the center manifold

$$(2.21) \quad \Phi = \sum_k \Phi_{0k} \mathbf{u}_{0k} + \sum_k \Phi_{2m,k} \mathbf{u}_{2m,k} + o(2),$$

Here

$$\Phi_K = \Phi_{1,K} x_1^2 + \Phi_{2,K} x_1 x_2 + \Phi_{3,K} x_2^2.$$

Using these results, the coefficients of the center manifold function can be computed as follows:

$$(2.22) \quad \begin{aligned} \Phi_{1,K} &= m_K^{-1} ((\beta_K^2 + 2 \operatorname{Im}(\beta)^2) g_K^{11} + 2 \operatorname{Im}(\beta)^2 g_K^{22} + \operatorname{Im}(\beta) \beta_K (g_K^{12} + g_K^{21})), \\ \Phi_{2,K} &= m_K^{-1} (\beta_K^2 (g_K^{12} + g_K^{21}) + 2 \operatorname{Im}(\beta) \beta_K (g_K^{22} - g_K^{11})), \\ \Phi_{3,K} &= m_K^{-1} ((\beta_K^2 + 2 \operatorname{Im}(\beta)^2) g_K^{22} + 2 \operatorname{Im}(\beta)^2 g_K^{11} - \operatorname{Im}(\beta) \beta_K (g_K^{12} + g_K^{21})). \end{aligned}$$

Using (2.18), (2.19) and (2.22), we find that

$$\begin{aligned} \Phi_{1,0k} &= \Phi_{3,0k}, \quad \Phi_{2,0k} = 0, \\ \Phi_{1,2m,k} &= \frac{i}{2} \Phi_{2,2m,k} = -\Phi_{3,2m,k} \end{aligned}$$

Hence the center manifold function (2.21) becomes

$$(2.23) \quad \Phi = \sum_k \Phi_{1,0k} \mathbf{u}_{0k} (x_1^2 + x_2^2) + \Phi_{1,2m,k} (x_1^2 - 2ix_1x_2 - x_2^2) \mathbf{u}_{2m,k} + o(2).$$

Note that $\Phi_{1,0k}$ is real while $\Phi_{1,2m,k}$ is complex.

Step 3. Construction of adjoint modes. Now we construct the adjoint modes \mathbf{U}^{*1} and \mathbf{U}^{*2} orthogonal to \mathbf{u}^1 and \mathbf{u}^2 . Let us denote the real and imaginary parts of the critical adjoint eigenvector by $\mathbf{u}^{*1} = \operatorname{Re} \mathbf{u}_{m_0,1}^*$ and $\mathbf{u}^{*2} = \operatorname{Im} \mathbf{u}_{m_0,1}^*$ and define

$$(2.24) \quad \mathbf{U}^{*1} = \frac{(\mathbf{u}^1, \mathbf{u}^{*1}) \mathbf{u}^{*1} + (\mathbf{u}^1, \mathbf{u}^{*2}) \mathbf{u}^{*2}}{(\mathbf{u}^1, \mathbf{u}^{*1})^2 + (\mathbf{u}^1, \mathbf{u}^{*2})^2}, \quad \mathbf{U}^{*2} = \frac{-(\mathbf{u}^1, \mathbf{u}^{*2}) \mathbf{u}^{*1} + (\mathbf{u}^1, \mathbf{u}^{*1}) \mathbf{u}^{*2}}{(\mathbf{u}^1, \mathbf{u}^{*1})^2 + (\mathbf{u}^1, \mathbf{u}^{*2})^2}.$$

Noting that for any two functions of the form $f_i(x, y) = e^{iam\pi x} g_i(y)$ for $i = 1, 2$ where m is a nonzero integer, we have

$$(\operatorname{Re} f_1, \operatorname{Re} f_2) = (\operatorname{Im} f_1, \operatorname{Im} f_2), \quad (\operatorname{Re} f_1, \operatorname{Im} f_2) = -(\operatorname{Im} f_1, \operatorname{Re} f_2).$$

Thus

$$(\mathbf{u}^1, \mathbf{u}^{*1}) = (\mathbf{u}^2, \mathbf{u}^{*2}), \quad (\mathbf{u}^1, \mathbf{u}^{*2}) = -(\mathbf{u}^2, \mathbf{u}^{*1}).$$

which implies that

$$(2.25) \quad \begin{aligned} (\mathbf{u}^2, \mathbf{U}^{*1}) &= (\mathbf{u}^1, \mathbf{U}^{*2}) = 0, \\ (\mathbf{u}^1, \mathbf{U}^{*1}) &= (\mathbf{u}^2, \mathbf{U}^{*2}) = 1. \end{aligned}$$

Step 4. Derivation of the reduced equations. Now we write

$$(2.26) \quad \mathbf{u}(x, y, t) = x_1(t)\mathbf{u}^1(x, y) + x_2(t)\mathbf{u}^2(x, y) + \Phi(x, y, t)$$

where Φ is the center manifold function, $x_1, x_2 \in \mathbb{R}$. Note that

$$L(\mathbf{u}^1 + i\mathbf{u}^2) = \beta(\mathbf{u}^1 + i\mathbf{u}^2)$$

implies

$$L\mathbf{u}^1 = \operatorname{Re}(\beta)\mathbf{u}^1 - \operatorname{Im}(\beta)\mathbf{u}^2, \quad L\mathbf{u}^2 = \operatorname{Re}(\beta)\mathbf{u}^2 + \operatorname{Im}(\beta)\mathbf{u}^1.$$

Also by definition of center manifold, we have $(\Phi, \mathbf{u}^{*1}) = 0$ and $(\Phi, \mathbf{u}^{*2}) = 0$ which by (2.24) implies that

$$(2.27) \quad (\Phi, \mathbf{U}^{*i}) = 0, \quad i = 1, 2.$$

Hence by (2.25) and (2.27)

$$(2.28) \quad \begin{aligned} (L\mathbf{u}, \mathbf{U}^{*1}) &= (x_1L\mathbf{u}^1, \mathbf{U}^{*1}) + (x_2L\mathbf{u}^2, \mathbf{U}^{*1}) = \operatorname{Re}(\beta)x_1 + \operatorname{Im}(\beta)x_2, \\ (L\mathbf{u}, \mathbf{U}^{*2}) &= (x_1L\mathbf{u}^1, \mathbf{U}^{*2}) + (x_2L\mathbf{u}^2, \mathbf{U}^{*2}) = \operatorname{Im}(\beta)x_1 + \operatorname{Re}(\beta)x_2. \end{aligned}$$

Plugging (2.26) into (2.3), taking inner product with \mathbf{U}^{*i} ($i = 1, 2$) and using (2.25) and (2.28), we can write the reduced equations as

$$(2.29) \quad \begin{aligned} \frac{dx_1}{dt} &= \operatorname{Re}(\beta)x_1 + \operatorname{Im}(\beta)x_2 + (G(\mathbf{u}, \mathbf{u}), \mathbf{U}^{*1}), \\ \frac{dx_2}{dt} &= -\operatorname{Im}(\beta)x_1 + \operatorname{Re}(\beta)x_2 + (G(\mathbf{u}, \mathbf{u}), \mathbf{U}^{*2}). \end{aligned}$$

Noting

$$G_s(\mathbf{u}^i, \mathbf{u}^j, \mathbf{U}^{*k}) = 0, \quad i, j, k = 1, 2,$$

and

$$G_s(\Phi, \Phi, \mathbf{U}^{*k}) = o(3).$$

we can expand the nonlinear terms of x_1 and x_2 in (2.29)

$$(2.30) \quad (G(\mathbf{u}, \mathbf{u}), \mathbf{U}^{*j}) = x_1G_s(\mathbf{u}^1, \Phi, \mathbf{U}^{*j}) + x_2G_s(\mathbf{u}^2, \Phi, \mathbf{U}^{*j}) + o(3).$$

By (2.23),

$$(2.31) \quad G_s(\mathbf{u}^i, \Phi, \mathbf{U}^{*j}) = \sum_k \Phi_{1,0k}(x_1^2 + x_2^2)c_{0k}^{ij} + \Phi_{1,2m,k}(x_1^2 - 2ix_1x_2 - x_2^2)c_{2m,k}^{ij},$$

where we define

$$(2.32) \quad \begin{aligned} c_{0,k}^{ij} &= G_s(\mathbf{u}^i, \mathbf{u}_{0k}, \mathbf{U}^{*j}), \\ c_{2m,k}^{ij} &= G_s(\mathbf{u}^i, \mathbf{u}_{2m,k}, \mathbf{U}^{*j}). \end{aligned}$$

As in (2.17), we can show that

$$(2.33) \quad \begin{aligned} c_{0k}^{11} &= c_{0k}^{22}, & c_{0k}^{12} &= -c_{0k}^{21}, \\ c_{2m,k}^{11} &= -c_{2m,k}^{22}, & c_{2m,k}^{12} &= c_{2m,k}^{21}. \end{aligned}$$

Moreover the calculation

$$(2.34) \quad \begin{aligned} G_s(\mathbf{u}^1, \mathbf{u}_{2m}^1, \mathbf{U}^{*1}) &= G_s(\mathbf{u}^1, \mathbf{u}_{2m}^2, \mathbf{U}^{*2}), \\ G_s(\mathbf{u}^1, \mathbf{u}_{2m}^2, \mathbf{U}^{*1}) &= -G_s(\mathbf{u}^1, \mathbf{u}_{2m}^1, \mathbf{U}^{*2}) \end{aligned}$$

implies that

$$(2.35) \quad c_{2m,k}^{11} = -ic_{2m,k}^{12}$$

Using (2.30)-(2.35), we have

$$(G(\mathbf{u}, \mathbf{u}), \mathbf{U}^{*j}) = b_{30}^j x_1^3 + b_{21}^j x_1^2 x_2 + b_{12}^j x_1 x_2^2 + b_{03}^j x_2^3 + o(3), \quad j = 1, 2,$$

where simple calculations show that

$$(2.36) \quad \begin{aligned} b_{30}^1 &= b_{12}^1 = b_{21}^2 = b_{03}^2 = \sum_k \Phi_{1,0k} c_{0k}^{11} + \Phi_{1,2m,k} c_{2m,k}^{11}, \\ b_{30}^2 &= b_{12}^2 = -b_{21}^1 = -b_{03}^1 = \sum_k \Phi_{1,0k} c_{0k}^{12} + i\Phi_{1,2m,k} c_{2m,k}^{11}. \end{aligned}$$

Thus the reduced equations (2.29) become

$$(2.37) \quad \begin{aligned} \frac{dx_1}{dt} &= \operatorname{Re}(\beta)x_1 + \operatorname{Im}(\beta)x_2 + b_{30}^1 x_1(x_1^2 + x_2^2) - b_{30}^2 x_2(x_1^2 + x_2^2) + o(3), \\ \frac{dx_2}{dt} &= -\operatorname{Im}(\beta)x_1 + \operatorname{Re}(\beta)x_2 + b_{30}^2 x_1(x_1^2 + x_2^2) + b_{30}^1 x_2(x_1^2 + x_2^2) + o(3). \end{aligned}$$

Step 5. Computation of the transition number γ . Letting $z = x_1 + ix_2$, (2.37) becomes

$$(2.38) \quad \frac{dz}{dt} = \bar{\beta}z + bz|z|^2 + o(|z|^3),$$

where by (2.35) and (2.36)

$$(2.39) \quad b = b_{30}^1 + ib_{30}^2 = \sum_k \Phi_{1,0k} (c_{0k}^{11} + ic_{0k}^{12})$$

If $\operatorname{Re} b < 0$ then (2.38) has a stable limit cycle

$$z = re^{i\omega t}$$

for $\operatorname{Re} \beta > 0$, i.e. for $R > R_0$ with

$$r = \sqrt{-\frac{\operatorname{Re} \beta}{\operatorname{Re} b}}, \quad \omega = -\operatorname{Im} \beta + \operatorname{Im} br^2 \approx -\operatorname{Im} \beta.$$

If $\operatorname{Re} b > 0$ then (2.38) has an unstable limit cycle for $R < R_0$.

Thus the transition is determined by the sign of real part of b in (2.39) at $R = R_0$ defined as

$$(2.40) \quad \gamma = \operatorname{Re}(b) = \sum_{k=1}^{\infty} \Phi_{1,0k} c_{0k}^{11}$$

since $\Phi_{1,0k}, c_{0k}^{11}, c_{0k}^{12}$ are real numbers.

Step 6. Derivation of the transition number γ in (2.10).

Using (2.18) in (2.22), we get

$$(2.41) \quad \Phi_{1,0k} = \frac{g_{0k}^{11}}{-\beta_{0k}(\mathbf{u}_{0k}, \mathbf{u}_{0k}^*)}$$

The mode $\mathbf{u}_{0k} = \mathbf{u}_{0k}^* = (\frac{\partial}{\partial y}\psi_{0k}, 0) = (DY_{0k}, 0)$ corresponds to the eigenfunction with $m = 0$ in (2.6), i.e. solutions of $ED^4Y = \beta D^2Y$ with the boundary conditions $Y(\pm 1) = D^2Y(\pm 1) = 0$. These solutions are easily obtainable.

$$(2.42) \quad \beta_{0k} = -\frac{k^2\pi^2}{4}E, \\ Y_{0k} = \begin{cases} \cos \frac{k\pi y}{2}, & \text{if } k \text{ is odd,} \\ \sin \frac{k\pi y}{2}, & \text{if } k \text{ is even.} \end{cases}$$

Thus

$$(\mathbf{u}_{0k}, \mathbf{u}_{0k}^*) = \frac{2}{a} \int_{-1}^1 |DY_{0k}|^2 = \frac{-2\beta_{0k}}{aE}.$$

To obtain γ , we need to compute

$$(2.43) \quad c_{0,k}^{11} = G_s(\mathbf{u}^1, \mathbf{u}_{0k}, \mathbf{U}^{*1}) = G(\mathbf{u}^1, \mathbf{u}_{0k}, \mathbf{U}^{*1}) + G(\mathbf{u}_{0k}, \mathbf{u}^1, \mathbf{U}^{*1})$$

and

$$(2.44) \quad g_{0k}^{11} = G(\mathbf{u}^1, \mathbf{u}^1, \mathbf{u}_{0k}^*)$$

where \mathbf{u}^1 is the real part of the critical eigenfunction (with zonal wave number m_0) as given in (2.12), \mathbf{U}^{*1} is given by (2.24) and G is the trilinear operator (2.13). So we plug in $\psi_{m_0 1} = e^{iam_0\pi x}Y_{m_0 1}(y)$ and $\psi_{m_0 1}^* = e^{iam_0\pi x}Y_{m_0 1}^*(y)$ into (2.43) and (2.44). After tedious computations, we can obtain

$$(2.45) \quad c_{0k}^{11} = -\frac{a\epsilon m_0\pi}{|J_1|^2} \text{Im}\{J_1 J_2(k)\}, \\ g_{0k}^{11} = -\frac{\epsilon m_0\pi\beta_{0k}}{E} \text{Im} J_3(k),$$

where

$$(2.46) \quad J_1 = \int_{-1}^1 \overline{Y^*}((am_0\pi)^2 - D^2)Y dy, \\ J_2(k) = \int_{-1}^1 DY_{0k}\overline{Y^*} \left((am_0\pi)^2 - \frac{k^2\pi^2}{4} - D^2 \right) Y dy, \\ J_3(k) = \int_{-1}^1 Y_{0k}Y D\overline{Y} dy.$$

Finally we note that $Y = Y_{m_0 1}$ is either an odd or an even function of y which follows from the fact that the equation (2.6) is invariant under the change of variable $y \rightarrow -y$. Thus Y_{0k} must be odd (by (2.42), k must be even) otherwise $J_3(k)$ is zero. So the nonzero contributions

to γ in (2.40) comes from even k . Thus we obtain (2.10) from (2.40), (2.41), (2.42), (2.45) and (2.46), which concludes the proof. \square

3. NUMERICAL EVALUATION

3.1. Legendre-Galerkin method for (2.6) and (2.7). In this section we present a method to approximate the solutions of the eigenvalue problems (2.6) and (2.7). There are fourth-order problems so a Legendre-Galerkin method [14, 15] will be efficient and accurate.

We look for an approximation of Y in the space $X_N = \{v \in P_N : v(\pm 1) = v''(\pm 1) = 0\}$, where P_N is the space of polynomials with degree less than or equal to N .

Using the approach in [14], we set

$$f_j(y) = L_j(y) + \sum_{k=1}^4 c_{j,k} L_{j+k}(y),$$

with $c_{j,k}$ to be chosen such that

$$f_j(\pm 1) = f_j''(\pm 1) = 0.$$

It is easy to determine from the properties of Legendre polynomials that

$$\begin{aligned} c_{j,1} &= c_{j,3} = 0, \\ c_{j,2} &= \frac{2(2j+5)(j^2+5j+9)}{(j+3)(j+4)(2j+7)}, \\ c_{j,4} &= -1 - c_{j,2}, \end{aligned}$$

and we have $X_N = \text{span}\{f_j : j = 0, 1, \dots, N-4\}$.

Writing $Y^N(y) = \sum_{j=0}^{N-4} y_j f_j(y) \in X_N$, and plugging it into (2.6), and taking inner product with $f_k(y)$, ($k = 0, 1, \dots, N-4$) we obtain the Legendre-Galerkin approximation of (2.6) in the following matrix form:

$$(3.1) \quad \begin{aligned} &\left(E(A_1 - 2\alpha_m^2 A_2 + \alpha_m^4 A_3) + i\alpha_m \left(\frac{R}{\pi^3} A_4^T + \frac{R}{\pi^3} (\pi^2 - \alpha_m^2) A_5 - A_3 \right) \right) \mathcal{Y}^N \\ &= \beta (A_2 - \alpha_m^2 A_3) \mathcal{Y}^N, \end{aligned}$$

where

$$\begin{aligned} a_{1,jk} &= (D^4 f_j, f_k), & a_{2,jk} &= (D^2 f_j, f_k), & a_{3,jk} &= (f_j, f_k), \\ a_{4,jk} &= (\cos \pi y D^2 f_j, f_k), & a_{5,jk} &= (\cos \pi y f_j, f_k) \\ A_i &= (a_{i,jk})_{j,k=0,\dots,N-4} \quad i = 1, \dots, 5 \\ \mathcal{Y}^N &= \begin{bmatrix} y_0 & y_1 & \cdots & y_{N-4} \end{bmatrix}^T. \end{aligned}$$

By using the properties of Legendre polynomials, we find that A_1, A_2, A_3 are real symmetric banded matrices given by

$$a_{1,jk} = \begin{cases} \frac{(2+2j)(2+j)(3+2j)^2(5+2j)}{(3+j)(4+j)}, & \text{if } j = k \\ 0, & \text{otherwise} \end{cases}$$

$$a_{2,jk} = \begin{cases} \frac{(2+2j)(2+j)(3+2j)}{(3+j)(4+j)}, & \text{if } j = k \pm 2 \\ \frac{(4(3+2j)(5+2j)(102+110j+47j^2+10j^3+j^4))}{(3+j)^2(4+j)^2(7+2j)}, & \text{if } j = k \\ 0, & \text{otherwise} \end{cases}$$

$$a_{3,jk} = \begin{cases} \frac{2(1+j)(2+j)(3+2j)}{(3+j)(4+j)(7+2j)(9+2j)}, & \text{if } j = k \pm 4 \\ \frac{-8(222+196j+77j^2+14j^3+j^4)}{(3+j)(4+j)(5+j)(6+j)(11+2j)}, & \text{if } j = k \pm 2 \\ \frac{4(5580+11202j+9263j^2+4170j^3+1105j^4+168j^5+12j^6)}{(3+j)^2(4+j)^2(1+2j)(7+2j)(9+2j)}, & \text{if } j = k \\ 0, & \text{otherwise} \end{cases}$$

To approximate A_4 and A_5 we fix some integer M and compute the Legendre-Gauss-Lobatto quadrature points y_n and weights ω_n for $n = 0, \dots, M$. Then we compute the matrices $D^2 f_j(y_n)$ and $f_j(y_n)$.

$$a_{4,jk} = \sum_{n=0}^M \cos(\pi y) D^2 f_j(y_n) f_k(y_n) \omega_n,$$

$$a_{5,jk} = \sum_{n=0}^M \cos(\pi y) f_j(y_n) f_k(y_n) \omega_n.$$

M is chosen large enough to provide sufficient accuracy in the computation of A_4 and A_5 . We note that A_4 and A_5 are real, full matrices. A_5 is symmetric while A_4 is non-symmetric.

The eigenvalue problem (3.1) can be easily solved by using a standard eigenvalue solver. For each $m \in \mathbb{Z}$, we can numerically find $N - 3$ eigenvalues $\beta_{m,j}^N$ (with $\text{Re } \beta_{m,j}^N \geq \text{Re } \beta_{m,k}^N$ if $j < k$) of (3.1), and corresponding eigenvectors $\mathcal{Y}_{m,j}^N$, $j = 1, \dots, N - 3$.

By taking the complex conjugate of (3.1), we find $\mathcal{Y}_{m,j}^N = \overline{\mathcal{Y}}_{-m,j}^N$, $\beta_{m,j}^N = \overline{\beta}_{-m,j}^N$ and in particular β_{0j}^N and ψ_{0j}^N are real.

It is known that ([16]), the computed eigenpairs $(\beta_{m,j}^N, e^{i\alpha_m x} Y_{m,j}^N)$ of (3.1) converge to eigenpairs $(\beta_{m,j}, \psi_{m,j})$ of (2.4) exponentially as $N \rightarrow \infty$ for $0 \leq j \lesssim 2N/\pi$ for each fixed m .

Finally, the analog of approximating equation (3.1) for the adjoint problem (2.7) is the adjoint problem of (3.1). Namely

$$(3.2) \quad \left(E(A_1 - 2\alpha_m^2 A_2 + \alpha_m^4 A_3) - i\alpha_m \left(\frac{R}{\pi^3} A_4 + \frac{R}{\pi^3} (\pi^2 - \alpha_m^2) A_5 - A_3 \right) \right) \mathcal{Y}^{*N} \\ = \beta^* (A_2 - \alpha_m^2 A_3) \mathcal{Y}^{*N}.$$

3.2. Numerical computation of the transition number γ . To approximate γ in (2.10), we follow the following steps:

Step 1 The parameters of the system are a , ϵ , E and R . We fix the Ekman number E and the length scale a . Then by (1.2), the Rossby number $\epsilon = R/E$ is also fixed. Moreover, to study the transition, R has to be fixed to $R = R_0$ where R_0 is determined by Assumption 1.

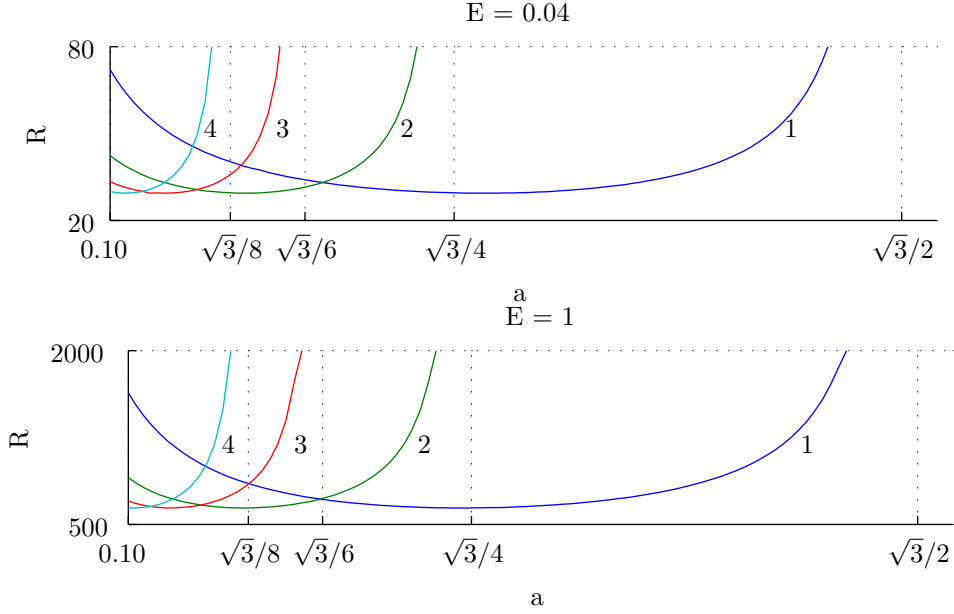


FIGURE 1. Neutral stability curves which are defined by $\text{Re } \beta_{m,1} = 0$ in the a - R plane for zonal wave numbers $m = 1, 2, 3, 4$ and for $E = 0.04, E = 1$.

Step 2 We determine the critical zonal wave number m_0 and the critical Reynolds number R_0 in Assumption 1. In [3], it was shown that $m_0 = 1$ if $\sqrt{3}/4 \leq a \leq \alpha_0$ for some $\alpha_0 < \sqrt{3}/2$. Figure 1 show that the difficulties in proving the Assumption 1 for $\alpha_0 \leq a < \sqrt{3}/2$ is purely technical. Extrapolating this result supported by our numerical computations of neutral stability curves shown in Figure 1, we claim that Assumption 1 can be satisfied by m only if $a < \sqrt{3}/(2m)$.

For such m , we set $\text{Re } \beta_{m,1}^N = 0$ in (3.1) and solve for the Reynolds number R to find $R_{0,m}^N$. R_0^N which approximates R_0 , is the minimum of such $R_{0,m}^N$ and the minimizing m value is m_0 .

Figure 1 shows that Assumption 1 holds for a simple complex pair of eigenvalues for almost all $a < \sqrt{3}/2$ except for discrete values of a where neutral stability curves corresponding to different zonal wave numbers intersect; Assumption 1 is generic.

Step 3 With $\beta_{m_0,1}^N$ computed, the eigensolutions $\mathcal{Y}_{m_0,1}^N = [\tilde{y}_j]_{j=0}^{N-4}$ and $\mathcal{Y}_{m_0,1}^{*N} = [\tilde{y}_j^*]_{j=0}^{N-4}$ of (3.1) and (3.2) are also found.

Step 4 The Legendre-Gauss-Lobatto quadrature points y_j and weights ω_j are calculated for $j = 0, \dots, M$ where M will be chosen large enough to allow sufficient accuracy in the computation of (3.3).

Step 5 The values of the eigenmodes and their derivatives at quadrature points y_j are computed.

$$Y_{m_0,1}^N(y_j) = \sum_{k=0}^{N-4} \tilde{y}_k f_k(y_j), \quad Y_{m_0,1}^{*N}(y_j) = \sum_{k=0}^{N-4} \tilde{y}_k^* f_k(y_j),$$

$$DY_{m_0,1}^N(y_j) = \sum_{k=0}^{N-4} \tilde{y}_k f'_k(y_j), \quad D^2 Y_{m_0,1}^N(y_j) = \sum_{k=0}^{N-4} \tilde{y}_k f''_k(y_j).$$

Step 6 It is easy to see that if we multiply $Y_{m_0,1}$ by a complex number c then γ is multiplied by $|c|^2$. To find a unique γ , we normalize $Y_{m_0,1}$ so that $\max_{0 \leq j \leq M} Y_{m_0,1}^N(y_j) = 1$.

Step 7 We can also normalize $Y_{m_0,1}^{*N}$ so that $I_1 = 1$ in (2.9). It is easy to see that this scaling has no effect on γ .

Step 8 Finally we approximate $I_2(k)$, $I_3(k)$ by

$$(3.3) \quad I_2(k) \approx \sum_{j=0}^M \cos(k\pi y_j) Y_{m_0,1}^{*N}(y_j) ((am_0\pi)^2 - k^2\pi^2 - D^2) \overline{Y_{m_0,1}^N(y_j)} \omega_j,$$

$$I_3(k) \approx \sum_{j=0}^M \sin(k\pi y_j) Y_{m_0,1}^N(y_j) \overline{DY_{m_0,1}^N(y_j)} \omega_j.$$

Obviously increasing M increases the accuracy of approximation in (3.3). In our experiments we found that $M = 2N$ gives enough accuracy.

3.3. Numerical results. In this section, we present the results of our numerical computations of γ for different parameter choices. As discussed in Section 3.2, the only parameters that need to be varied are the Ekman number E and the length scale a .

For showing typical results, we consider a mid-latitude atmospheric jet in a zonal channel at a reference latitude $\theta_0 = 45^\circ\text{N}$. The dimensional zonal velocity of the background state u_0 in (1.4) has a maximum $U/(\pi^3 E)$. With a typical zonal velocity of $U = 15 \text{ ms}^{-1}$, we limit our numerical investigations to E values between 0.01 to 0.03 which corresponds to maximum zonal jet velocities between 16 ms^{-1} up to 48 ms^{-1} . For $a = 0.2$, a typical length scale of $L = 3000 \text{ km}$ yields a channel of length $2L/a = 30000 \text{ km}$ in the meridional direction that corresponds to about 360° in longitude. We therefore consider a values in the range $0.1 \leq a \leq 0.6$.

For this parameter regime we approximate the transition number γ following the procedure in Section 3.2. The results we find are presented in Table 1 which suggest that γ is always positive. According to Theorem 1, this means the transition is Type-II at the first critical Reynolds number R_0 .

We can also compute the period $T = 2\pi/\text{Im}\beta_{m_0,1}$ of the solution (2.11) where T has been non-dimensionalized by $1/(\beta_0 L)$. For example, with the above choices of L and U , for $a = 0.20$ and $E = 0.01$ we find that $m_0 = 2$, $R_0 = 5.64$. The planetary vorticity gradient β_0 at 45°N is 1.6×10^{-11} . We compute the period to be about $T = 196$ days. The stream function of the time periodic solution (2.11) bifurcated on $R < R_0$ which is unstable because of the Type-II transition is shown in Figure 2. The pattern indicates a typical one due to barotropic instability which, due to the background state zonal velocity, propagates eastwards.

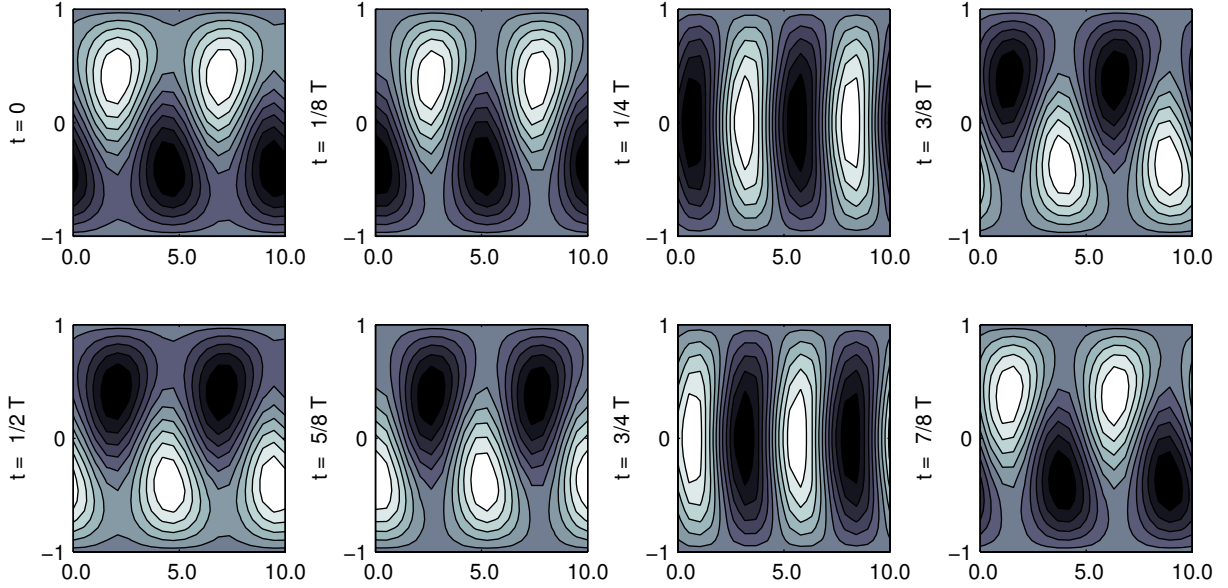


FIGURE 2. The stream function of the bifurcated periodic solution on $R < R_0$ at $a = 0.2$ and $E = 0.01$; T denotes the period of the periodic orbit.

TABLE 1. The value of γ for $0.1 \leq a \leq 0.6$ and $0.01 \leq E \leq 0.03$.

		a					
		0.100	0.200	0.300	0.400	0.500	0.600
E	0.010	0.197	0.197	0.188	0.197	0.194	0.175
	0.015	0.174	0.174	0.163	0.174	0.172	0.155
	0.020	0.156	0.156	0.143	0.156	0.156	0.143
	0.025	0.144	0.144	0.130	0.144	0.146	0.135
	0.030	0.135	0.135	0.121	0.135	0.139	0.130

4. SUMMARY AND DISCUSSION

In this paper, we have extended the results of [3] on the existence of a Hopf bifurcation in the forced barotropic vorticity equation (1.1) by rigorously showing the type of finite amplitude solutions which can occur near this Hopf bifurcation. Central in the analysis is the computable quantity γ which characterizes the transition behavior near the critical point.

The aim of this paper was only to focus on the theory and numerical computation. As an illustration, we explore this number numerically in a parameter regime relevant for an atmospheric jet and find that a catastrophic transition is preferred. For typical ocean cases,

for example in western boundary currents such as the Gulf Stream and the Kuroshio, and the Antarctic Circumpolar Current, the results will be reported elsewhere.

While (1.1) is a cornerstone dynamical model of the ocean and atmospheric circulation, it of course represents only a limited number of processes. As practiced by the earlier workers in this field, such as J. Charney and J. von Neumann, and from the lessons learned by the failure of Richardson's pioneering work, one tries to be satisfied with simplified models approximating the actual motions to a greater or lesser degree instead of attempting to deal with the atmosphere/ocean in all its complexity. By starting with models incorporating only what are thought to be the most important of atmospheric influences, and by gradually bringing in others, one is able to proceed inductively and thereby to avoid the pitfalls inevitably encountered when a great many poorly understood factors are introduced all at once.

However, the same results will be true if we work on the barotropic equations in primitive variables; see (2.2) and [12]. Second, we would expect that the same type of results obtained in this article will also be true if we use higher order friction (e.g. hyper-friction, [13]) in (1.1) as this would only change the eigenfunction structure slightly. Third, the method presented in this paper combined with the methods introduced in [1, 2] can be used to study the case with bottom topography [4], and the case where noise represents ocean eddies. We will explore these new directions in the near future.

Acknowledgment. The work of H.D. was supported by the Netherlands Organization for Scientific Research (NWO) through the COMPLEXITY project PreKurs; the work of T.S. was supported by the Scientific and Technological Research Council of Turkey (Grant number 114C142); the work of J.S. was partially supported by NSF grants DMS-1217066 and DMS-1419053; and the work of S.W. was supported in part by NSF grant DMS-1211218.

REFERENCES

- [1] M. CHEKROUN, H. LIU, AND S. WANG, *Approximation of Invariant Manifolds: Stochastic Manifolds for Nonlinear SPDEs I*, Springer Briefs in Mathematics. Springer, New York, 2014.
- [2] ———, *Parameterizing Manifolds and Non-Markovian Reduced Equations: Stochastic Manifolds for Nonlinear SPDEs II*, Springer Briefs in Mathematics. Springer, New York, 2014.
- [3] Z.-M. CHEN, M. GHIL, E. SIMONNET, AND S. WANG, *Hopf bifurcation in quasi-geostrophic channel flow*, SIAM J. Appl. Math., 64 (2003), pp. 343–368 (electronic).
- [4] D. T. CROMMELIN, J. D. OPSTEEGH, AND F. VERHULST, *A mechanism for atmospheric regime transitions*, J. Atmos. Sci., 61 (2004), p. 14061419.
- [5] H. DIJKSTRA, *Nonlinear Climate Dynamics*, Cambridge Univ. Press, Cambridge, UK, 2013.
- [6] H. A. DIJKSTRA, *Nonlinear Physical Oceanography: A Dynamical Systems Approach to the Large Scale Ocean Circulation and El Niño.*, Kluwer Academic Publishers, Dordrecht, the Netherlands, 2000.
- [7] H. A. DIJKSTRA AND M. GHIL, *Low-frequency variability of the large-scale ocean circulations: a dynamical systems approach*, Review of Geophysics, 43 (2005), pp. 1–38.
- [8] M. GHIL, *Is our climate stable? bifurcations, transitions and oscillations in climate dynamics, in science for survival and sustainable development, v. i. keilis-borok and m. snchez sorondo (eds.), pontifical academy of sciences, vatican city, (2000)*, pp. 163–184.
- [9] IPCC, 2013, *Climate Change 2013: The Physical Science Basis. Contribution of Working Group I to the Fifth Assessment Report of the Intergovernmental Panel on Climate Change (IPCC) [Stocker, T.F. et al. (eds)]*, Cambridge University Press, Cambridge, UK and New York, NY, 2013. Also available from www.ipcc.ch.
- [10] T. MA AND S. WANG, *Phase Transition Dynamics*, Springer-Verlag, 2013.
- [11] J. PEDLOSKY, *Geophysical Fluid Dynamics*, Springer-Verlag, New-York, second ed., 1987.
- [12] T. SAPSIS AND H. A. DIJKSTRA, *Interaction of additive noise and nonlinear dynamics in the double-gyre wind-driven ocean circulation*, J. Phys. Oceanography, 43 (2013), pp. 366–381.

- [13] F. M. SELTEN, *An efficient description of the dynamics of barotropic flow*, Journal of the Atmospheric Sciences, 52:7 (1995), p. 915936.
- [14] J. SHEN, *Efficient spectral-Galerkin method I. direct solvers for second- and fourth-order equations by using Legendre polynomials*, SIAM J. Sci. Comput., 15 (1994), pp. 1489–1505.
- [15] J. SHEN, T. TANG, AND L.-L. WANG, *Spectral methods*, vol. 41 of Springer Series in Computational Mathematics, Springer, Heidelberg, 2011. Algorithms, analysis and applications.
- [16] J. A. C. WEIDEMAN AND L. N. TREFETHEN, *The eigenvalues of second-order spectral differentiation matrices*, SIAM J. Numer. Anal., 25 (1988), pp. 1279–1298.

(HD) INSTITUTE FOR MARINE AND ATMOSPHERIC RESEARCH UTRECHT DEPARTMENT OF PHYSICS AND ASTRONOMY UTRECHT UNIVERSITY PRINCETONPLEIN 5, 3584 CC UTRECHT, THE NETHERLANDS
E-mail address: H.A.Dijkstra@uu.nl

(TS) DEPARTMENT OF MATHEMATICS, YEDITEPE UNIVERSITY, 34750 ISTANBUL, TURKEY
E-mail address: taylansengul@gmail.com

(JS) DEPARTMENT OF MATHEMATICS, PURDUE UNIVERSITY, WEST LAFAYETTE, IN 47907
E-mail address: shen7@purdue.edu

(SW) DEPARTMENT OF MATHEMATICS, INDIANA UNIVERSITY, BLOOMINGTON, IN 47405
E-mail address: showang@indiana.edu, <http://www.indiana.edu/~fluid>